15TH IEA HEAT PUMP CONFERENCE
MAY 26–29, 2026 | HOFBURG
VIENNA 2026
DECARBONISATION THROUGH INNOVATION

Optimum discharge pressure correlation based on experimental data for R744 direct expansion ground source heat pump in space heating applications

Minghan Xu[a,b,*], Parham Eslami-Nejad[a,c]

[a]CanmetENERGY Research Centre (Varennes), Natural Resources Canada, Varennes QC, Canada
[b]Department of Civil and Mineral Engineering, University of Toronto, Toronto ON, Canada
[c]Vitalis equipment technology, Kelowna BC, Canada

Abstract

Optimum discharge pressure control in a transcritical carbon dioxide direct expansion ground source heat pump (CO_2-DX-GSHP) can further improve the system's thermal performance. To achieve the highest coefficient of performance (COP) possible, accurate and reliable correlations based on empirical data are essential. These correlations ensure the optimum operation of CO_2-DX-GSHP systems. The literature offers several correlations for transcritical CO_2 systems using numerical models for air-source and water heating applications; however, only a few have developed correlations for space heating based on experimental data. In this study, the optimum discharge pressure of a CO_2-DX-GSHP was evaluated experimentally for space heating. For this purpose, a fully instrumented CO_2-DX-GSHP test bench at CanmetENERGY Research Centre was used. Several polynomial-based correlations are then formulated for the system's COP over a wide range of discharge pressure and for specific supply and return water temperatures suitable for space heating applications. Results indicate that the COP could be improved by 50% compared to cases without optimal control for the space heating application.

Keywords: Direct expansion ground source heat pump, CO_2, space heating, optimum discharge pressure, correlation.

1. Introduction

Utilizing carbon dioxide (CO_2, or R744) as a refrigerant in heat pumps has attracted significant attention as the technology upgrade addresses environmental concerns and complies within stringent refrigerant regulations [1]. In addition to its low environmental impact, CO_2 offers unique thermophysical properties advantageous for water heating and low-temperature thermal applications [2,3]. The higher operating pressure and favorable heat transfer characteristics of CO_2 also enable smaller pipe diameters, lower mass flow rates, and reduced pressure drops compared to conventional refrigerants in ground heat exchangers (GHE) [4,5]. Consequently, integrating CO_2 with ground source heat pump (GSHP) technology offers a more promising and sustainable system configuration.

Most studies on transcritical CO_2 heat pumps have focused on modeling and numerical optimization of the coefficient of performance (COP) through discharge pressure control. Existing correlations typically express the optimum discharge pressure $P_{dis,opt}$ as a function of the gas cooler outlet temperature [6,7]. However, experimental studies on optimum pressure control remain limited. A few investigations have explored air-source and water-heating systems [8,9], but no work has been performed to experimentally analyze the optimum discharge pressure of CO_2 direct expansion in GSHP systems for space heating. To address this gap, the present study experimentally investigates the optimum discharge pressure of a CO_2-DX-GSHP system under controlled operating conditions. Key parameters such as evaporating and superheat temperatures are

* Corresponding author. *E-mail address:* minghan.xu@utoronto.ca

15th IEA Heat Pump Conference 2026 - IGS4.5 - https://doi.org/10.23697/52sq-hz65

precisely controlled, and empirical correlations for COP are developed for specific supply and return water temperatures suitable for space heating applications.

2. System Description

For this study, a fully instrumented laboratory test bench is used to evaluate experimentally the optimum discharge pressure of a CO_2-DX-GSHP. The schematic of the experimental design is presented in Figure 1. The setup is designed primarily to measure thermal performance under various thermodynamic conditions. As shown in Figure 1, the experimental apparatus is equipped with a gas cooler, a CO_2 reservoir, a CO_2 compressor, an internal heat exchanger (IHE), two expansion valves (EV), and a pressure regulating valve (PR). The heat generated in the gas cooler is taken using a semi-chiller. A constant-temperature water bath (CTB) and a water-to-CO_2 heat exchanger supply heat to the system when the capacity of GHE is insufficient. Expansion valves (EV1 and EV2) are used to set suction and discharge pressures in the system. Specifically, EV1 is used to adjust the evaporating temperature (suction pressure), while EV2 is installed to set the discharge pressure. There is also an IHE to supply enough superheat at the compressor suction. The compressor is fixed-speed with a displacement of 1.35 m³/h. The CTB (downstream from the GHE) compensates for the energy required to complete evaporation and maintains desired suction pressure (evaporating temperature). The test setup is fully instrumented on both the CO_2 and water sides to measure the thermal/electric energy going in-and-out of the system. The capacity of the system is rated at 1.5 ton refrigeration (5.3 kW at 5°C evaporating temperature, 80 bar discharge pressure, and 25°C gas cooler outlet temperature).

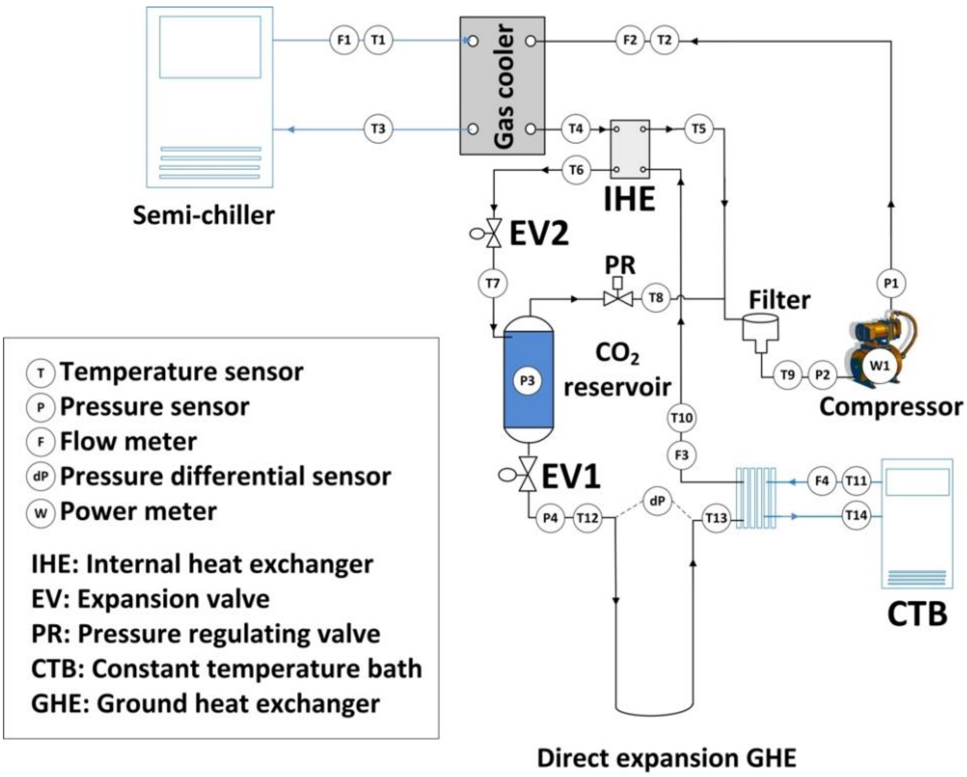

Figure 1. Schematic of the experimental system.

3. Methodology

3.1. Experimentation

To evaluate the system's optimum discharge pressure, the following steps were taken:

- The opening of EV1 is set to get the desired evaporating temperature (which in turn mimics the GHE operation), and the superheat temperature is measured and controlled at the IHE.

- The water temperature and flow rate entering the gas cooler from the semi-chiller are also set to fix the outlet water temperature, $T_{gc}^{o,w}$, exiting the gas cooler. In this study, a temperature differential of 8°C between the water inlet and outlet is chosen to mimic space heating application. In this condition, temperature difference between water entering the gas cooler and CO2 exiting the gas cooler changes in the range of 3°C to 5°C.
- EV2 is set to control a given discharge pressure.

Using temperature sensors at both the gas cooler's inlet and outlet on the water side, the gas cooler heat transfer rate, $\dot{Q}_{gc}$, is measured as follows:

$$\dot{Q}_{gc} = \dot{m}^w c_p^w \left(T_{gc}^{o,w} - T_{gc}^{i,w}\right) \quad (1)$$

where $\dot{m}^w$, c_p^w, $T_{gc}^{o,w}$, and $T_{gc}^{i,w}$ are the water mass flow rate, specific heat capacity, and gas cooler outlet and inlet water temperatures, respectively. Furthermore, the compressor's power consumption is measured using a power meter, and the heat pump's coefficient of performance, COP, is calculated by the following equation:

$$COP = \frac{\dot{Q}_{gc}}{\dot{W}_{comp}} \quad (2)$$

where $\dot{W}_{comp}$ is the power consumed by the compressor.

The discharge pressure is changed from 71 to 94 bars to account for the variations in the water inlet temperature. Enough time is spent at each discharge pressure to stabilize the operation. Then, the desired test parameters are recorded to calculate the heat pump's $\dot{Q}_{gc}$ and COP. Furthermore, during each test, the evaporating temperature is set using a fixed expansion valve (EV1) opening. Though air source heat pumps operate as low as −20°C under cold climates, the operational temperature for the GSHP is much higher due to the fact that the ground temperature is around 10°C. For this reason, the optimum pressure for this application have been evaluated for three different evaporating temperatures in the range of system operation from -5°C to 3°C. Lastly, the superheat temperature is regulated to a fixed value in all scenarios, at 18.5 ± 0.5°C (recommended to be at least 15°C by the compressor manufacturer). Each test required 1 to 2 hours to be perfectly stabilized after the controlled parameters were set. The data recording for each test was done 15 minutes after stabilization, thus allowing an accurate and reliable measurement of the data.

3.2. Uncertainty analysis

An uncertainty analysis was performed using root sum square (RSS). Specifically, the uncertainties of the outlet water temperature from the gas cooler, $T_{gc}^{o,w}$, evaporating temperature, T_{ev}, heating capacity, $\dot{Q}_{gc}$, and COP, are calculated to determine the accuracy of the optimum pressure determined based on the measurements. The $T_{gc}^{o,w}$ is measured using an RTD temperature sensor with a relatively high precision of 0.15°C at the given temperature range ($\delta T_{gc}^{o,w}$ = ±0.15°C). The T_{ev} is calculated from the measured evaporating pressure, P_{ev}, at its saturation, as the pressure sensor has a higher accuracy than a surface thermocouple installed on the CO_2 pipe at the evaporator inlet. To evaluate the uncertainty of the T_{ev} from the P_{ev}, a relationship between the saturation temperature and pressure is required. At saturation, the following relationship between T_{sat} (°C) and P_{sat} (bar) can be found (by fitting the data from [10]):

$$T_{sat} = -0.017P_{sat}^2 + 2.38P_{sat} - 61.97 \quad (3)$$

which is valid for −40°C ⩽ Tsat ⩽ 20°C, applicable for the T_{ev} and the P_{ev} in this study. The uncertainty of the T_{ev} can therefore be obtained as follows:

$$\delta_{T_{ev}} = \pm\sqrt{\left(\frac{\partial T_{ev}}{\partial P_{ev}}\delta P_{ev}\right)^2} \quad (3)$$

Similar approaches are used for the uncertainties of $\dot{Q}_{gc}$ and COP.

4. Results and Discussion

4.1. Experimental measurements and uncertainties

In this subsection, a set of data for specific $T_{gc}^{i,w}$ and T_{ev} is presented as an example to demonstrate the measurements and uncertainties in the experimentation. Notably, 17 tests were carried out in this study at various discharge pressures within the range from 75 to 91 bars under the condition of $T_{gc}^{i,w}$ = 32°C and T_{ev} = 0.75°C. The outlet water temperature from the gas cooler, $T_{gc}^{o,w}$, was carefully adjusted at the beginning of each test by varying the water mass flow rate in a range from 0.095 to 0.173 L/s. In figure 2, it is rather clear to see that the heating capacity increases as the discharge pressure rises, whereas the COP reaches its maximum at approximately 87 bars. The specific value of the maximum COP, i.e., the optimum operating point, requires uncertainty analysis and mathematical correlation, a procedure that will be discussed in the subsequent subsections.

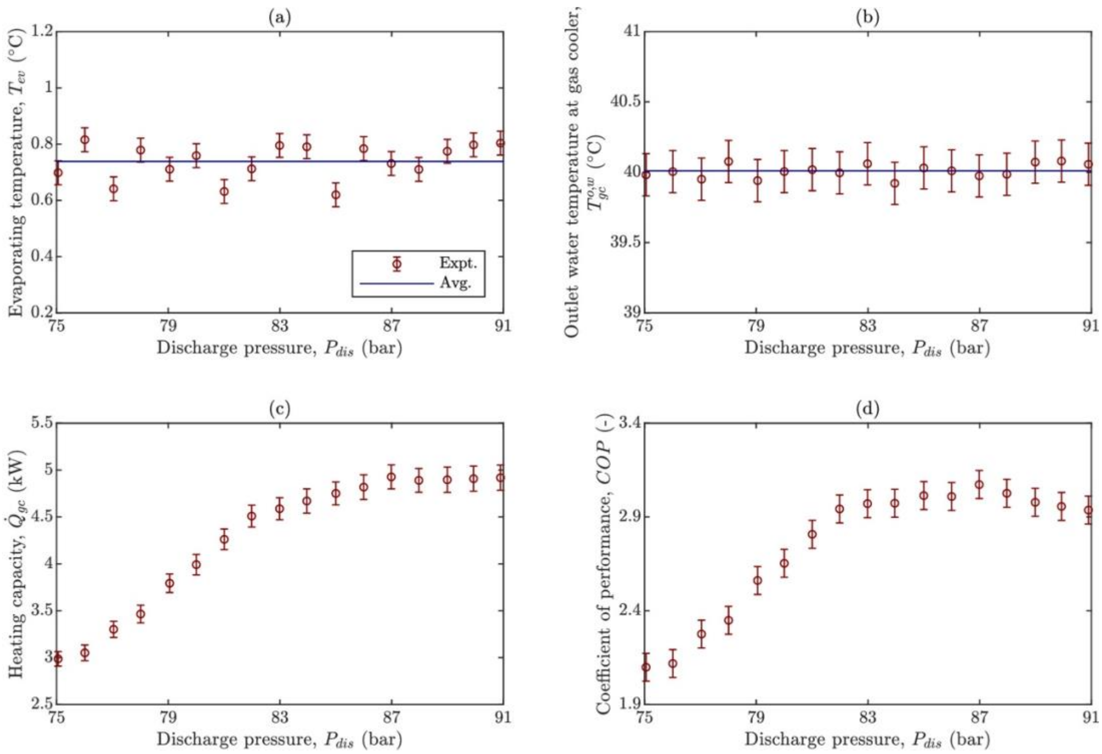

Figure 2. Experimental measurements with calculated uncertainty: (a) T_{ev}, (b) $T_{gc}^{o,w}$, (c) $\dot{Q}_{gc}$, and (d) COP.

Figures 2(a,b) present the evaporating temperature and the outlet water temperature for different discharge pressures with calculated uncertainties. The T_{ev} is set by the expansion valve (EV1) to a desired value. Then, the T_{ev} is determined using the evaporating pressure, P_{ev}. The uncertainty of the T_{ev} is calculated using the pressure-temperature correlation in saturation as expressed in Eq. (3). Consequently, the averaged uncertainty of the T_{ev} is calculated as ±0.04°C for the pressure sensor's given accuracy. The uncertainty of the $T_{gc}^{o,w}$ is considered to be ±0.15°C, as it is directly measured using the RTD and the average value is approximately 40°C. Figures 2(c,d) present the $\dot{Q}_{gc}$ and COP values for various discharge pressures, P_{dis}, along with their uncertainties. The uncertainties of $\dot{Q}_{gc}$ and COP are calculated based on Eq. (5) and Eq. (6), for an average of ±0.12 kW and ±0.08, respectively.

4.2. Correlations of coefficient of performance over discharge pressure

The experimental measurements of the COP for various discharge pressures demonstrate an optimum system operation in terms of energy consumption and geothermal exchange for a desired heating requirement. As discussed previously in Section 1, there is limited research on the optimal control of these systems for space heating applications. Hence, it is valuable to develop a correlation for these systems and applications based on the experimental data obtained in this study.

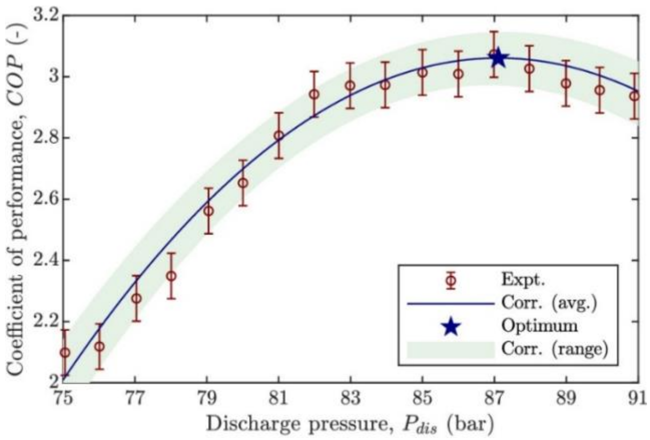

Figure 3. COP over the discharge pressure P_{dis} for $T_{gc}^{i,w}$ = 32°C and T_{ev} = 0.75°C (experimental data and a corresponding correlation).

The correlation between the COP and the discharge pressure, P_{dis}, derived using polynomials, is presented in Figure 3. Three correlations (minimum, average, and maximum) are established to account for instrumental uncertainties. These correlations are expressed as a piecewise function, which is provided below:

$$COP = \begin{cases} -7.86 \times 10^{-3} P_{dis}^2 + 1.36 P_{dis} - 56.23, for\ minimum \\ -7.17 \times 10^{-3} P_{dis}^2 + 1.25 P_{dis} - 51.34, for\ average \\ -6.72 \times 10^{-3} P_{dis}^2 + 1.17 P_{dis} - 47.97, for\ maximum \end{cases} \quad (1)$$

where P_{dis} is in bars. The valid range for these correlations is 75 bars $\leqslant$ P_{dis} $\leqslant$ 91 bars, and the optimum discharge pressure based on the averaged correlation is $(P_{dis})_{opt}$ $\approx$ 87.11 bars with a maximum COP of 3.06. Accounting for uncertainties, the optimum discharge pressure, $(P_{dis})_{opt}$, varies from 86.87 to 87.24 bars, while the maximum COP has a span of 2.97 $\leqslant$ $(COP)_{opt}$ $\leqslant$ 3.15. The percent deviations for the $(P_{dis})_{opt}$ and $(COP)_{opt}$ are calculated as 0.22% and 2.8%, respectively. It is worth noting that the deviation of the optimum COP is much higher than that of the optimum discharge pressure since many factors could influence the COP. Further analysis to quantify the impact of evaporating temperature on the optimum COP will be presented in the following subsection. It is also clear that the optimum COP can reach over three at the optimum discharge pressure (i.e., 87.11 bars), which is approximately 50% higher than the COP at 75 bars.

4.3. Effect of evaporating temperature

Another critical parameter for CO2-DX-GSHP systems is the evaporating temperature, T_{ev}. During system operation for space heating, the evaporating temperature decreases over time as the ground temperature drops close to the GHE. It is, therefore, crucial to assess how the evaporating temperature affects the optimal pressure. Figure 4 illustrates the effect of the T_{ev} by fixing the inlet and outlet water temperatures to be 32°C and 40°C, respectively, while evaluating the COP at different P_{dis}. This study selected T_{ev} values of –5°C, 0.75°C, and 3°C to represent the range of changes in T_{ev} under undisturbed ground temperatures ranging from 5°C to 13°C, which are typical of most regions in Canada. The uncertainty and corresponding correlations for each T_{ev} are performed in the same approach as in Fig. 3. As shown, the optimum discharge pressure hardly changes across evaporation temperatures. The maximum deviation is determined to be within 2 bars. Considering the costs associated with control, it may not be essential to adjust the discharge pressure for each ground heat extraction condition, as long as the inlet and outlet water temperatures remain constant. On the other hand, the optimum COP increases significantly with the T_{ev}. For instance, as the evaporating temperature increases from –5°C to 3°C, the optimum COP rises by approximately 30%.

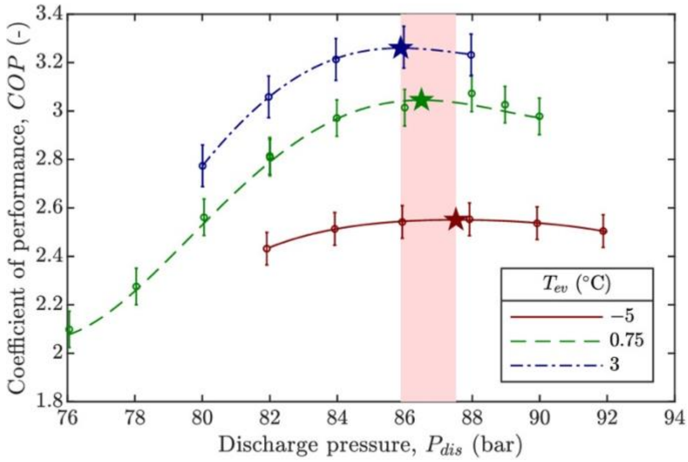

Figure 4. COP over P_{dis} for various evaporating temperatures and fixed water inlet temperature of 32°C (experimental data and corresponding correlations).

5. Conclusion

In this research, a laboratory-scale CO_2 direct expansion ground source heat pump (CO_2-DX-GSHP) was used to determine the optimum discharge pressure of the system for space heating applications. Several important parameters, including inlet and outlet water temperatures, evaporating temperature, and superheat temperature, were carefully controlled to ensure that the impact on the COP and the system capacity was solely driven by the discharge pressure. Uncertainty analysis was also performed to evaluate the accuracy of the measured and calculated results. It is recommended that future works include further investigations on the effect of system characteristics and applications on the optimum discharge pressure through numerical modelling and potential development of a universal correlation for CO_2 transcritical heat pump systems operating in heating mode regardless of the system characteristics.

References

[1] P. Neksa, CO2 heat pump systems, International Journal of Refrigeration 25 (4) (2002) 421– 427. Van der Geer J, Hanraads JAJ, Lupton RA. The art of writing a scientific article. *J Sci Commun* 2000;**163**:51–9.
[2] J. Zhang, Y. Qin, C. Wang, Review on CO2 heat pump water heater for residential use in japan, Renewable and Sustainable Energy Reviews 50 (2015) 1383–1391.
[3] P. Bansal, A review–status of CO2 as a low temperature refrigerant: Fundamentals and r&d opportunities, Applied Thermal Engineering 41 (2012) 18–29.
[4] P. Eslami-Nejad, A. Nguyen, M. Cimmino, A. Bastani, M. Badache, Performance comparison of a vertical direct expansion geothermal evaporator: Part I, single U-pipe using different refrigerants, International Journal of Refrigeration 116 (2020) 119–128.
[5] P. Eslami-Nejad, M. Cimmino, A. Nguyen, M. Badache, A. Bastani, Performance comparison of a vertical direct expansion geothermal evaporator: Part II, multiple U-pipes, International Journal of Refrigeration 116 (2020) 161-171.
[6] S. Liao, T. Zhao, A. Jakobsen, A correlation of optimal heat rejection pressures in transcritical carbon dioxide cycles, Applied Thermal Engineering 20 (9) (2000) 831–841.
[7] J. Sarkar, S. Bhattacharyya, M. R. Gopal, Optimization of a transcritical CO2 heat pump cycle for simultaneous cooling and heating applications, International Journal of Refrigeration 27 (8) (2004) 830–838.
[8] S. Wang, H. Tuo, F. Cao, Z. Xing, Experimental investigation on air-source transcritical CO2 heat pump water heater system at a fixed water inlet temperature, International Journal of Refrigeration 36 (3) (2013) 701–716.
[9] P. Qi, Y. He, X. Wang, X. Meng, Experimental investigation of the optimal heat rejection pressure for a transcritical CO2 heat pump water heater, Applied Thermal Engineering 56 (1-2) (2013) 120–125.

[10] I. H. Bell, J. Wronski, S. Quoilin, V. Lemort, Pure and pseudo-pure fluid thermophysical property evaluation and the open-source thermophysical property library CoolProp. Industrial & Engineering Chemistry Research 53 (6) (2014) 2498–2508.